Solution-Processible Small Molecular Organic Light-Emitting Diode Material and Devices Based on the Substituted Aluminum Quinolate

Jung-An Cheng,† Chin H. Chen,*,‡ and Chi Hung Liao†

Department of Applied Chemistry, and Display Institute, Microelectronics and Information System Research Center, National Chiao Tung University, Hsinchu, Taiwan 30050

Received December 11, 2003. Revised Manuscript Received May 19, 2004

We have discovered a new type of small molecular host material based on aluminum(III) 8-hydroxyquinolates, $Al(Saq)_3$, which was synthesized with three 5-(*N*-ethylanilinesulfonamide)-8- quinolinoline as bidentate ligands. By X-ray diffraction crystallographic analysis, the crystals of meridional $Al(Saq)_3$ are monoclinic, space group $P2_1/c$, $a = 17.952(3)$ Å, $b = 17.716(3)$ Å, $c = 17.080(3)$ Å, $\beta = 99.895(4)°$. Its peak photoluminescence in solid phase appears at 488 nm. Its LUMO/HOMO (−3.13/−6.04 eV) and optical band gap (E_g 2.91 eV) were determined by cyclic voltammetry . In solid thin film morphological investigation, it shows good thermal properties and high quantum efficiency. When doped with 0.7 wt % of the high fluorescent green dopant 10-(2-benzothiazolyl)-1,1,7,7-tetramethyl-2,3,6,7-tetrahydro-1*H*,5*H*,11*H*-benzo-[*l*]pyrano[6,7,8-ij]quinolizin-11-one (C-545T), energy transfer from $Al(Saq)_3$ to dopant will occur and high green light emission can be achieved. For fabrication of OLEDs using spin-coating techniques, its electroluminescence is at 1931 $CIE_{x,y}$ (0.21, 0.41).

Introduction

Since high-efficiency small-molecule-based heterojunction organic light-emitting diodes (OLEDs) were reported by Tang et al. in 1987,[1] most of the small-molecule-based OLEDs have been fabricated by multilayer vacuum thermal evaporation techniques. Because of the relative ease of synthesis, purification, and RGB color-control by chromophoric design, small molecules of guest−host dopant systems based on Alq_3 are particularly suitable for fabrication of full-color OLEDs[2] and commercialization of this technology is well underway.[3] On the other hand, solution-processed small-molecule OLEDs are rare except for some large dendriatic molecules,[4] polymers,[5] and oligomers.[6] Therefore, development of fabrication technology of OLEDs via solution-processible small-molecule materials would offer an attractive alternative to vacuum techniques and also open up the exciting possibilities of fabrication similar to that demonstrated in PLEDs.[7]

One of the most attractive features of organic EL devices, relative to inorganic devices, is the ability to easily tune the emission wavelength by modifying substituents in organic materials. In the aluminum(III) complex of 8-hydroxyquinoline (Alq_3), placing electron-withdrawing substituents in C-5 of the quinoline ring is predicted to increase the energy difference between the highest occupied molecular orbital (HOMO) and the lowest unoccupied molecular orbital (LUMO).[8,9] This kind of host with larger energy gap will enhance its capacity to sensitize various singlet dopants to achieve full color emission with higher efficiency. 8-Hydroxy-5-quinolinesulfonate esters would appear to be one of the attractive functional groups for these properties, since the corresponding precursor, 8-hydroxyquinoline-5-sulfonyl chloride,[10] is known and can be readily synthesized.[11] However, quinolinesulfonate esters are relatively rare and unstable compared to other aromatic sulfonate esters.[12] Sulfonamide substituents offer greater stability and retain the electron-withdrawing character of the sulfonate substituent.

In this paper, we report the discovery of a new type of small-molecule host material—hereby abbreviated as $Al(Saq)_3$—for fabrication of OLEDs using spin-coating

* Corresponding author. Tel: +886-3-5712121 #59200. Fax: +886-3-5737681. E-mail: fredchen@mail.nctu.edu.tw.
† Department of Applied Chemistry.
‡ Display Institute, Microelectronics and Information System Research Center.

(1) Tang, C. W.; VanSlyke, S. A. *Appl. Phys. Lett.* **1897**, *51*, 913.
(2) Tang, C. W.; VanSlyke, S. A.; Chen, C. H. *J. Appl. Phys.* **1989**, *65*, 3610.
(3) Rajeswaran, G.; Itoh, M.; Boroson, M.; Barry, S.; Hatwar, T. K.; Kahen, K. B.; Yoneda, K.; Yokoyama, R.; Yamada, T.; Komiya, N.; Kanno, H.; Takahashi, H. *SID '00 Digest* **2000**, ISSN0000-0966X/00/3101-0974.
(4) Markham, J. P. J.; Lo, S.-C.; Magennis, S. W.; Burn, P. L.; Samuel, I. D. W. *J. Appl. Phys.* **2002**, *80*, 2645.
(5) Male, N. A. H.; Salata, O. V.; Christou, V. *Synth. Met.* **2002**, *126*, 7.
(6) Crispin, A.; Crispin, X.; Fahlman, M.; Cornil, J.; Johansson, N.; Bauer, J.; Weissortel, F.; Salbeck, J.; Bredas, J. L.; Salaneck, W. R. *J. Chem. Phys.* **2002**, *116*, 8159.
(7) Haskal, E. I.; Buechel, M.; Sempel, A.; Heeks, S. K.; Athanassopoulou, N.; Carter, J. C.; Wu, W.; O'Brien, J.; Fleuster, M.; Visser, R. J. *Asia Display/IDW '01*; Society for Information Display: San Jose, CA, 2001; OEL2-2, p 1411.
(8) Chen, C. H.; Shi, J. *Coord. Chem. Rev.* **1998**, *171*, 161.
(9) Albright, T. A.; Burdett, J. K.; Whangbo, M.-H.; *Orbital Interactions in Chemistry*; Wiley: New York, 1985.
(10) Yanni, A. S.; Abdel-Hafez, A. A.; Moharram, A. M. *J. Ind. Chem. Soc.* **1990**, *67*, 487.
(11) Hopkins, T. A.; Meerholz, T. K.; Shaheen, S.; Anderson, M. L.; Schmidt, A,; Kippelen, B.; Padias, A. B.; Hall, H. K.; Peyghambarian, N., Jr.; Armstrong, N, R. *Chem. Mater.* **1996**, *8*, 344.
(12) *Jpn. Kokai Tokkyo Koho* JP 5877, 864.

10.1021/cm035313i CCC: $27.50
Published on Web 07/02/2004

Scheme 1. Synthesis of Al(Saq)$_3$ Complex: (i) Chlorosulfonic Acid; (ii) *N*-ethylaniline/ Triethylamine/CH_2Cl_2; (iii) Triethylaluminum/THF

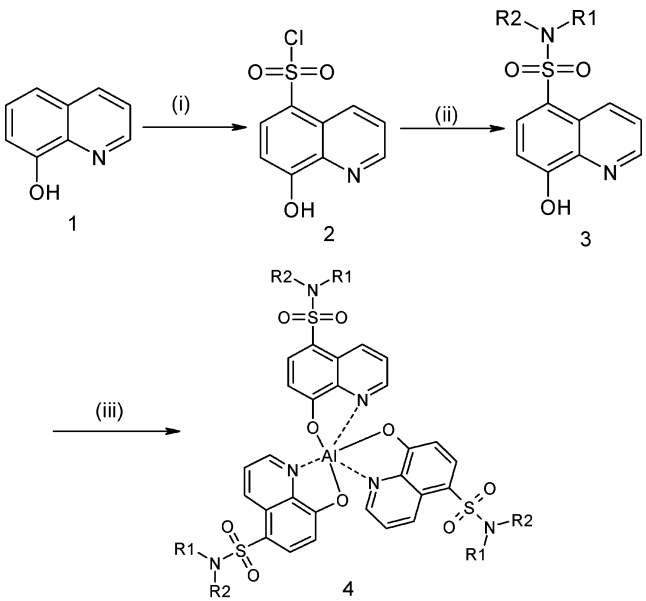

techniques. According to Scheme 1, 5-(*N*-ethyl-*N*′-phenyl-sulfonamide)-8-quinolinoline as bidentate ligands can be synthesized from commercially available 8-hydroxyquinoline.[10] By molecular design, the six-coordinated aluminumquinolate with sulfonate substituents can be used as wide band gap host materials ($E_g \approx 2.9$ eV) for various singlet dopants to tune the emission and efficiency of OLEDs.

Experimental Section

^{1}H NMR was recorded with a Varian Unity-300 Hz spectrometer. Elemental analysis was obtained by using a Heraeus CHN−OS Rapid analyzer. PL and EL spectra were carried out by Acton Research Spectra Pro-150 and PhotoResearch PR-650, respectively. Optical absorption was measured by a Hewlett Packard 8453 absorption spectrometer. The thermal properties of Al(Saq)$_3$ was determined by means of thermogravimetric analysis (TGA) and differential scanning calorimetry (DSC).

8-Hydroxyquinoline-5-*N*-ethylanilinesulfonamide (3). In a 100-mL round-bottom flask fitted with a magnetic stirrer, condenser, and N_2 inlet were placed 8-hydroxyquinoline-5-sulfonyl chloride (**2**)[10] (2.00 g, 8.21 mmol) with 10 mL of dichloromethane. Triethylamine (3.41 mL), *N*-ethylaniline (1.17 g, 9.85 mmol), and dichloromethane (10 mL) mixtures were added slowly into the reactor. The suspension was heated to reflux for 24 h. The reaction solution was filtered, and the solid byproduct was also removed. Solvent was stripped off by rotary vapor and the solid was sublimed at 2.0×10^{-2} mm Torr at 150 °C. White crystals were collected to yield 2.15 g (80%). ^{1}H NMR (300 MHz, $CDCl_3$) δ 8.774 (1H, dd, J = 4.4 Hz); 8.530 (1H, d, J = 11.1 Hz); 8.109 (1H, dd, J = 8.4 Hz); 7.364 (1H, dd, J = 4.2 Hz); 7.335 (1 H, dd, J = 4.2 Hz); 7.188−7.262 (2H, m); 7.146 (1H, dd, J = 8.1 Hz); 7.006 (2H, d, J = 8.3 Hz); 3.643 (2 H, q); 1.077 (3H, t). Mp 136−137 °C. IR (KBr) 3288 (br), 3057, 2970, 2929, 2868, 1622, 1572, 1509, 1493, 1336, 1285, 1202, 1149, 1060, 958 cm^{-1}. The product was characterized by mass spectrum which revealed no extraneous peak other than the desired parent m/e = 328 (M^+); 329 ($M^+ + 1$) (for $C_{17}H_{16}N_2O_3S$). Anal. Calcd for $C_{17}H_{16}N_2O_3S$: C, 62.18; H, 4.91; N, 8.53; O, 14.62; S, 9.76. Found: C, 62.31; H, 5.04; N, 8.44.

Tris(5-*N*-ethylanilinesulfonamide-8-quinolato-N_1,O_8)-aluminum (4). A 200-mL flask fitted with an N_2 inlet, septum, and stir bar was flame-dried and cooled under N_2. Compound **3** (1.00 g, 3.05 mmol) was added along with 60 mL of anhydrous THF. A hexane solution of triethylaluminum (1.11 mL, 15 w/w %) was added via syringe. A yellow solution with blue-green fluorescence was immediately visible. The reaction was stirred at room temperature for 48 h. Solvent was stripped off and the volatile impurities present in the remaining yellow residue were removed by vacuum sublimation to give 0.95 g (95%) of **4**. ^{1}H NMR (300 MHz, $CDCl_3$) δ 8.51−8.73 (6 H, m); 7.83 (3 H, t); 6.88−7.38 (21 H, br); 3.42−3.75 (6 H, br); 1.000−1.087 (9 H, m). Mp 192−193 °C. T_g = 143 °C. T_d = 372 °C (weight loss at 5 wt %). The product **4** was characterized by mass spectrum which revealed no extraneous peak other than the desired parent m/e = 1010. IR (KBr) 3467 (br), 3098, 3057, 3011, 2975, 2924, 2868, 1603, 1567, 1498, 1463, 1393, 1373, 1335, 1229, 1168, 1147, 1091, 1060, 978, 891 cm^{-1}. Anal. Calcd for $C_{51}H_{48}N_6O_9S_3Al$: C, 60.70; H, 4.49; N, 8.33; O, 14.27; S, 9.53; Al, 2.67. Found: C, 60.28; H, 4.72; N, 8.45.

X-ray Diffraction. A suitable yellow crystal with dimensions of 0.20 × 0.10 × 0.05 mm^3 was selected for indexing and intensity data collection on a Siemens SMART CCD diffractometer equipped with a normal-focus, 3-kW sealed-tube X-ray source. Intensity data were collected at room temperature in 1271 frames with ω scans (width 0.30° per frame). Empirical absorption corrections based on symmetry equivalents were applied ($T_{min,\ max}$ = 0.816, 0.952)[13] of the 38142 reflections collected ($2\theta_{max}$ = 56.56°), 2594 unique reflections were considered observed [$I > 2\sigma - (I)$] after data reduction. The structure was solved by direct methods: the Al atom was first located and the O, S, C, and N atoms in the framework were found in difference Fourier maps. There are four Al(Saq)$_3$ molecules per unit cell. The final cycles of least-squares refinement included atomic coordinates and anisotropic thermal parameters for all non-hydrogen atoms. The final difference Fourier maps were flat ($\Delta\rho_{max,min}$ = 0.61, −0.37 e/Å^3). All calculations were performed using the SHELXTL Version 5.1 software package.[14] Figure 1 shows the final Rietveld refinement plot. A summary of crystal data and refinement parameters can be found in Table 1.

Photoluminescence. For the solution investigation, the compound was dissolved in 1,2-dichloroethane ($c = 10^{-3}$−10^{-4} mol/L). For the solid-phase investigations of the pure compounds, thin films of 1,2-dichloroethane solution (4 wt %) were spin-coated. UV−Vis absorption spectra were measured with a HP spectrophotometer by using either the solutions in cuvettes of 10-mm path length or the solid thin film coated on quartz plates. The PL spectra were recorded with an Acton Research Spectra Pro-150 spectrometer. For the PL experiments, the excitation wavelength was set at the absorption maximum of the complex.

Device Fabrication. The three different device structures, ITO/PEDOT:PSS/Al(Saq)$_3$ blend/LiF/Al, were prepared in the following manner for EL measurement. For all structures the indium−tin-oxide (ITO, sheet resistance is 20 Ω//□) glass substrates were cleaned ultrasonically with detergent, deionized water, 2-propanol, and methanol. After cleaning, poly(3,4-ethylenedioxythiophene)/poly(styrene)-sulfonate (PEDOT:PSS, obtained from Bayer) aqueous solution was spin-coated at 3000 rpm onto the cleaned ITO substrates and baked at 110 °C for 4 h. Neat Al(Saq)$_3$ or blend LEDs were subsequently spin-coated on the PEDOT layer at 2500 rpm to give films typically 70 nm thick; a 1-nm layer of lithium fluoride (LiF) and a 200-nm layer of Al were sequentially deposited at 1×10^{-6} Torr. The emitting area of the device was 3 mm × 3 mm. The voltage−current−luminance characteristics were measured using an optical power meter (PR-650) and digital source meter (Keithley 2400). The EL spectra were measured under ambient atmosphere after encapsulation.

(13) Sheldrick, G. M. *SADABS*; Siemens Analytical X-ray Instrument Division: Madison, WI, 1995.
(14) Sheldrick, G. M. SHELXTL Programs, version 5.1; Bruker AXS Gmbh: Karlsruhe, Germany, 1998.

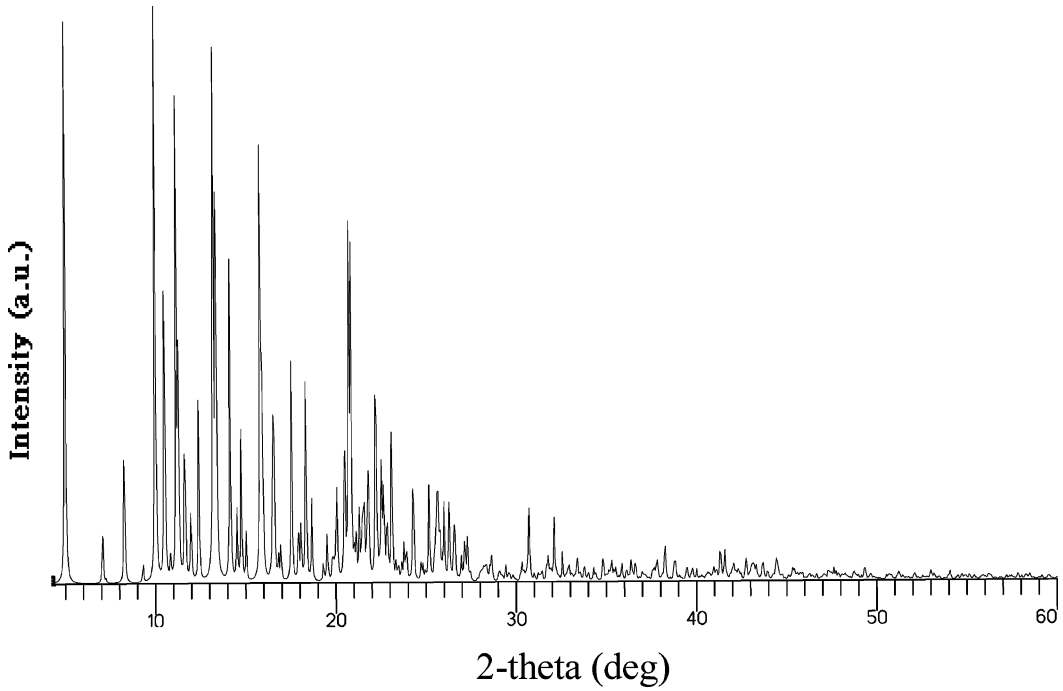

Figure 1. Rietveld refinement plot of the X-ray diffraction pattern of the $Al(Saq)_3$ phase. Calculated profiles and peak markers are shown.

Table 1. Crystal Data and Summary of Intensity Data Collection and Structure Refinement

	$Al(Saq)_3$
empirical formula	$C_{51}H_{45}AlN_6O_9S_3$
fw	1009.14
temp, K	294(2)
wavelength, Å	0.71073
cryst syst	monoclinic
space group	$P2_1/c$
unit cell dimensions	
a (Å)	17.952(3)
b (Å)	17.716(3)
c (Å)	17.080(3)
β (deg)	99.895(4)
vol, Å^3	5351.5(16)
Z	4
density (calcd), mg/m^3	1.292
ABS coeff, mm^{-1}	0.215
F(000)	2184
θ range for data collection, deg	1.15 to 28.28
index ranges	$-18 \le h \le 23$
	$-23 \le k \le 22$
	$-22 \le l \le 21$
reflns collected	38142
indep reflns	13232 [R(int) = 0.3427]
refinement method	full-matrix least-squares on F^2
data/restraints/parameters	13232/0/652
GOF on F^2	0.615
Final R indices	0.0592[a]
wR2	0.1296[b]

[a] $R1 = \sum|F_o| - |F_c|/\sum|F_o|$. [b] $wR2 = \{\sum[w(F_o^2 - F_c^2)^2]/\sum[w(F_o^2)^2]\}^{1/2}$, $w = 1/[\sigma^2(F_o^2) + (aP)^2 + bP]$, P] $[\mathrm{Max}(F_o,0) + 2(F_c)^2]/3$, where a = 0.0474 and b = 6.44.

Results and Discussion

Synthesis and Characterization of $Al(Saq)_3$ Complex. An aluminum(III) complex, $Al(Saq)_3$, with three 5-(*N*-ethyl-*N*′-phenyl-sulfonamide)-8-quinolinoline (**3**) as bidentate ligands was synthesized as shown in Scheme 1. Commercially available 8-hydroxyquinoline was reacted with chlorosulfonic acid to afford 5-chlorosulfonyl-8-hydroxyquinoline (**2**) which was reacted further with *N*-ethylaniline to obtain 8-hydroxyquinoline-5-*N*-ethylanilinesulfonamide (**3**). It was found that compound **3** is easily hydrolyzed with silica gel during purification by column chromatography. Therefore, it was purified by controlled sublimation to avoid side reaction. Finally, reacting ligand **3** with triethylaluminum produced a total yield of more than 64% of the desired six-coordinated Alq_3 derivative. In general, six-coordinated aluminum (III) complexes are often prepared by using aluminum chloride or aluminum alkoxide to chelate 8-hydroxyquinolines. But in our synthesis, sulfonamide groups introduced at C-5 of the bidentate ligand were sensitive to pH. If this kind of aluminum (III) salts were used as reagents, side products will be produced at the expense of decreasing yield and purity. Compared to a similar synthesis reported by Hopkins et al.,[11] this synthesis is not only simpler to prepare, but also higher in yield. In regard to solubility, it was known that poor solubility often reacts in ligands when sulfonamide groups were introduced to 8-hydroxyquinoline at C-5.[10,12] In our study, we varied amide groups to improve solubility in common organic solvents. Initially, we added different amines, such as R_1=R_2=phenyl and R_1=phenyl, R_2=H, on the sulfonyl group. Although the solubility was improved, it was still not as good as that of $Al(Saq)_3$. Therefore, the improvement in the solubility of the complex is insignificant by capping the *N*-ethylamine on sulfonyl group. The complex is soluble in commercially available solvents such as 1,2-dichloroethane, THF, dimethylforamide (DMF), and dimethyl sulfoxide (DMSO).

Description of the Structure. The single-crystal structure of molecules and relative information in bond lengths and angles are important for understanding intermolecular interaction, fluorescence, and molecular film characteristics. It's shown by X-ray diffraction that $Al(Saq)_3$ is a tris-chelate organometallic complex in which the metal atom (Al) has a distorted octahedral coordination. Figure 2 shows the molecular plot of Al-

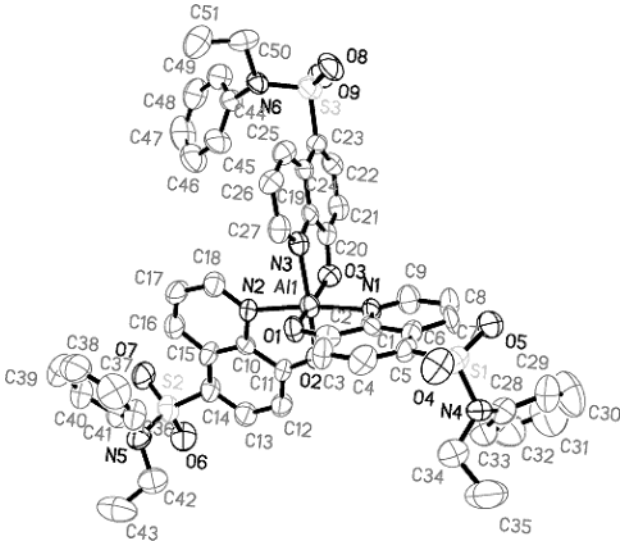

Figure 2. ORTEP drawings of $Al(Saq)_3$. The thermal ellipsoids represent a 50% probability limit. Hydrogen atoms are omitted for clarity.

Table 2. Selected Bond Distances (Å) and Angles (deg) for $Al(Saq)_3$ and Alq_3

	$Al(Saq)_3$	Alq_3[16]
	Bond Distances (Å)	
Al(1)−O(2)	1.844(5)	1.849(3)
Al(1)−O(1)	1.849(5)	1.863(3)
Al(1)−O(3)	1.855(6)	1.858(3)
Al(1)−N(1)	2.034(6)	2.033(4)
Al(1)−N(2)	2.047(6)	2.035(4)
Al(1)−N(3)	2.068(7)	2.078(4)
O(1)−C(2)	1.344(8)	1.317(5)
O(2)−C(11)	1.310(8)	1.318(5)
O(3)−C(20)	1.322(8)	1.322(5)
	Angles (deg)	
O(1)−Al(1)−N(1)	82.7(3)	83.0(2)
O(2)−Al(1)−N(2)	83.0(3)	83.9(1)
O(3)−Al(1)−N(3)	81.7(3)	71.7(1)
N(1)−Al(1)−N(2)	172.9(3)	173.2(2)
N(1)−Al(1)−N(3)	94.0(2)	92.4(1)
N(2)−Al(1)−N(3)	91.4(3)	90.6(1)

$(Saq)_3$, and crystallographic data are given in Table 1.[15] It can exist in either of the two geometrical isomers: the "meridional" (C_1 symmetry) isomer or the "facial" (C_3 symmetry) isomer, which differ in the relative positions of the oxygens and nitrogens of the metal coordination shell. In X-ray diffraction analysis, the meridional form was obtained. The determined crystal structures and solid-state packing of $Al(Saq)_3$ are very similar to Alq_3 in which it crystallizes in the monoclinic space group $P2_1/c$ with a unit cell content of four formula units. Three oxygen atoms and an aluminum atom form the equatorial plane and three nitrogen atoms occupy the apical positions. Three molecules of the bidentate ligand, 8-hydroxyquinoline-5-*N*-ethylanilinesulfonamide, are therefore coordinated to the aluminum. The selected bond lengths (Å) and angles (deg) for $Al(Saq)_3$ and Alq_3 are presented in Table 2. The average distance of Al−O and Al−N bonds are 1.849 and 6.149 Å, respectively. The average bond angle of O−Al−N is 82.5°. In comparison, these bond lengths and angles listed in Table 2 are almost the same as those of the Alq_3 chemical structure in the literature.[16]

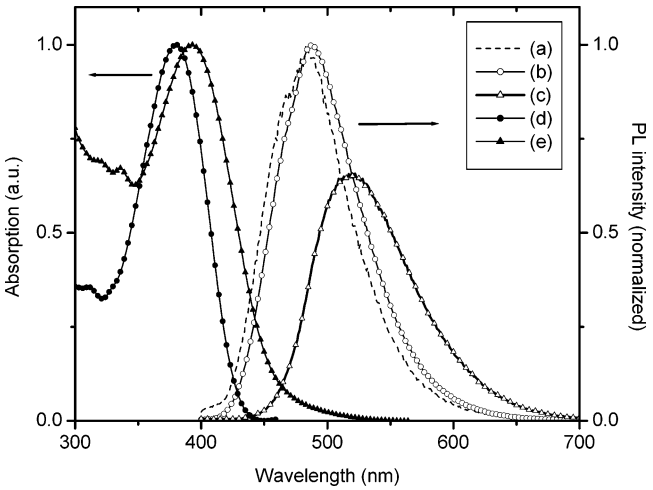

Figure 3. Comparison of optical properties of $Al(Saq)_3$ and Alq_3. Photoluminescence spectra: (a) $Al(Saq)_3$ in 1,2-dichloroethane, (b) $Al(Saq)_3$ thin solid film, and (c) Alq_3 thin solid film. UV−Vis absorption: (d) $Al(Saq)_3$ thin solid film, and (e) Alq_3 thin solid film.

Table 3. Absorption and Photoluminescence Results for Solutions and Films of Alq_3 and $Al(Saq)_3$

	solution investigation			solid film investigation		
	ABS λ_{max} (nm)	PL λ_{max} (nm)	Stokes shift (nm)	ABS λ_{max} (nm)	PL λ_{max} (nm)	Stokes shift (nm)
Alq_3[a]	390	514	124	393	519	126
$Al(Saq)_3$[b]	382	483	101	382	488	106

[a] The solid thin films were made by thermal deposition. [b] The solid thin films were made by spin-coating.

Absorption and Photoluminescence (PL). The normalized absorption and PL spectra (with excitation at the absorption maximum) obtained from thin films of Alq_3 and $Al(Saq)_3$ as the pure compounds are shown in Figure 3. By regiospecific derivatization of Alq_3 at one of its LUMO sites of C-5, sulfonamide groups removing electron density to the phenol ring will result in an increase in the energy of the $\pi-\pi^*$ transition which hypsochromic shifts the emission of Alq_3 to the blue.[8] Solutions were also investigated in 1,2-dichloroethane. The maximum absorption and emission wavelengths are summarized in Table 3. Their relative positions are 382/483 nm, in solution, and 382/488 nm, in solid, respectively. As expected, the introduction of the sulfonamide substituent to the C-5 of the quinoline ring system leads to blue-shifts of 8 and 31 nm in the absorption and emission maximums, respectively, of 1,2-dicholoethane solutions of $Al(Saq)_3$ as compared to those of Alq_3. The same blue shift was also observed in absorption and emission maximums (11 and 31 nm) in thin film phase. This shift is consistent with the electron-withdrawing nature of the sulfonamide substituent. The Stokes shift of $Al(Saq)_3$ is smaller than that of Alq_3 due to the lower intermolecular packing between $Al(Saq)_3$ molecules which suppresses the formation of excimers between molecules.

Net Thin Films of $Al(Saq)_3$ Formed by Solution Process. Figure 4 shows the atomic force microscope (AFM) image of the solid thin film coated from 3 wt %

(15) Cheng, J. A.; Chan, C. C.; Chen, C. H.; Chen, J. F. *Anal. Sci.* **2004**, *20*, 37.

(16) Fujii, I.; Hirayama, N.; Ohtani, J.; Kodama, K. *Anal. Sci.* **1996**, *12*, 153.

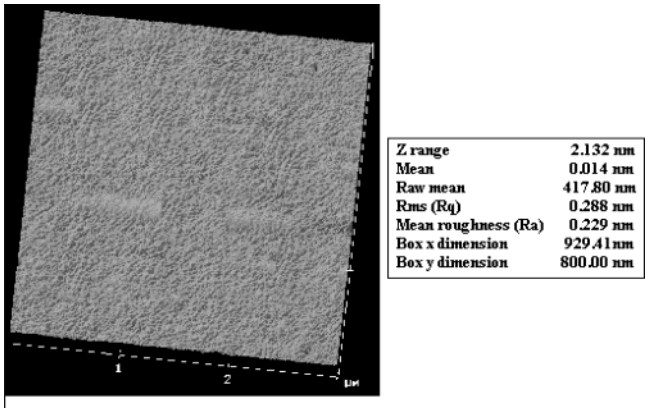

Figure 4. AFM image of $Al(Saq)_3$ thin film, spin-coated from 1,2-dichloroethane.

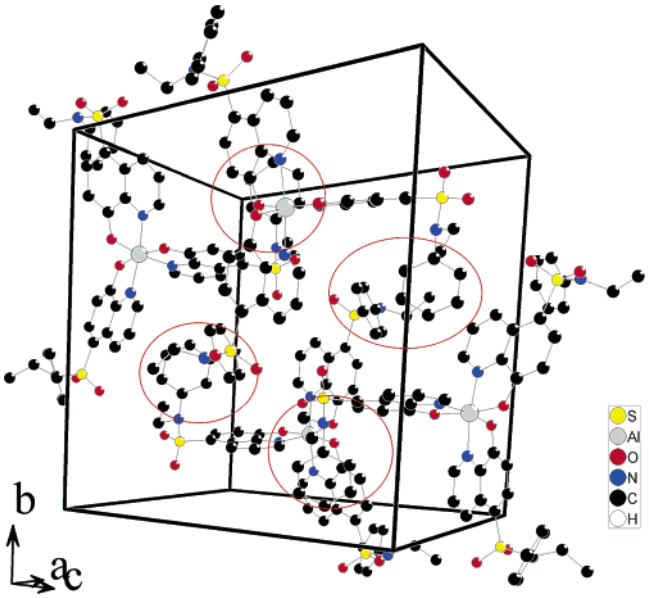

Figure 5. Crystal packing of $Al(Saq)_3$ based on the X-ray diffraction pattern. There are four molecules in the unit cell.

$Al(Saq)_3$ in 1,2-dichloroethane. The AFM image reveals that the film was pinhole free. Its root mean square (rms) and mean roughness (R_a) are 0.288 and 0.229 nm, respectively. Thin film phase prepared by spin-coating is presumably possible for most small molecular materials due to formation of intermolecular hydrogen bonding or physical entanglement. For understanding the mechanism of thin film formation, molecular packing from X-ray is shown in Figure 5. The intermolecular forces are mainly from the packing of sulfonamide groups at C-5 of quinolate ring. The intermolecular distance of adjacent phenyl rings in sulfonamide group is estimated at 3.4 Å (as shown by the circle). Because of the hook-like nature of sulfonamide group at C-5, the molecules of $Al(Saq)_3$ are randomly dispersed in the solvent matrix. The intermolecular hook-like sulfonamide groups will be tangled physically and form physical bonding. Therefore, thin film phase could be formed very well on ITO glass or silicon wafer via spin coating. The adhesion of these films on substrates was also tested to be relatively strong by using the stick-tape test.

In addition, from the packing diagram it is clear that the formation of $Al(Saq)_3$ crystalline is caused by the packing of phenyl rings on the sulfonamide. However, the density of the packing of phenyl rings in the globular

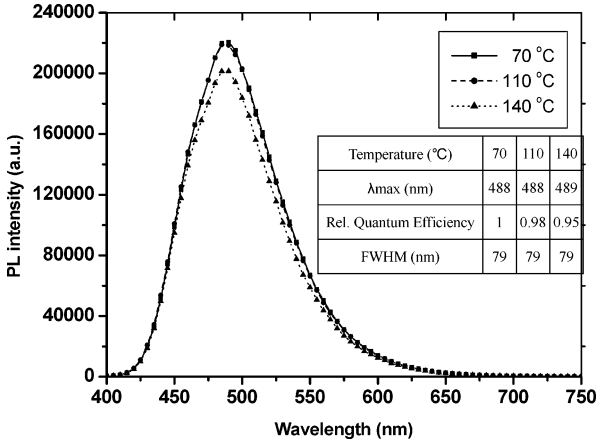

Figure 6. Solid PL of $Al(Saq)_3$ annealing at various temperatures for 48 h.

complex is low. Therefore, when the film is spin-coated on the substrate using solution process method, crystallization of $Al(Saq)_3$ by intermolecular phenyl ring packing is difficult. Figure 6 shows the PL of $Al(Saq)_3$ solid thin films after annealing for 48 h at temperatures of 70, 110, and 140 °C. The structure of $Al(Saq)_3$ solid film phase can suppress intermolecular packing and aggregation. It is clear from the graph that λ_{max} values at different temperatures do not change (488−489 nm), and the quantum efficiency has dropped 5% at 140 °C. These phenomena can be explained by the differential scanning calorimetry (DSC) measurement shown in Figure 7, which shows that the melting point peak at 190−200 °C was absent during the first heating step, and the recrystalization peak was absent as well as during the first cooling step. The result is the same as those in the second heating and cooling step. Under an optical microscope with polarizer, recrystallization phenomena of the sample were not observed during the heating and cooling process. Because the annealing temperature (140 °C) is very close to the T_g of $Al(Saq)_3$ (T_g = 143 °C), small vibronic motion of molecules will be expected under this temperature. A long period of annealing will cause intermolecular rearrangement, but because sulfonamide is hook-like, it will suppress orderly intermolecular arrangement. Here, the full width at half-maximum (fwhm) of PL spectra for three thin films are the same as 79 nm. All of the phenomena showed the formation of $Al(Saq)_3$ crystalline is not easy and most of the solid $Al(Saq)_3$ exists as amorphous state.

Study of Host−Guest Energy Transfer. In various studies of host−guest system, we found that various ratios of 10-(2-benzothiazolyl)-1,1,7,7-tetramethyl-2,3,6,7-tetrahydro-1*H*,5*H*,11*H*-benzo-[*l*]pyrano[6,7, 8-ij]quinolizin-11-one (abbreviated as C-545T) blended into $Al(Saq)_3$ produced good quantum efficiency. As shown in Figure 8, the excited $Al(Saq)_3$ could transfer its energy to C-545T by Förster energy-transfer in solid films. When C-545T was doped into $Al(Saq)_3$, the most prominent peak at 489 nm was quenched and replaced by the sharper narrow emission at λ_{max} 521 nm of C-545T. The energy transfer is optimized when 0.75 wt % of C-545T is doped into $Al(Saq)_3$. Its relative quantum yield is 1.75 times that of neat $Al(Saq)_3$ film under the integral area of PL curves. The quantum efficiency has improved and a more saturated green light with 1931 $CIE_{x,y}$ (0.31, 0.65) is observed.

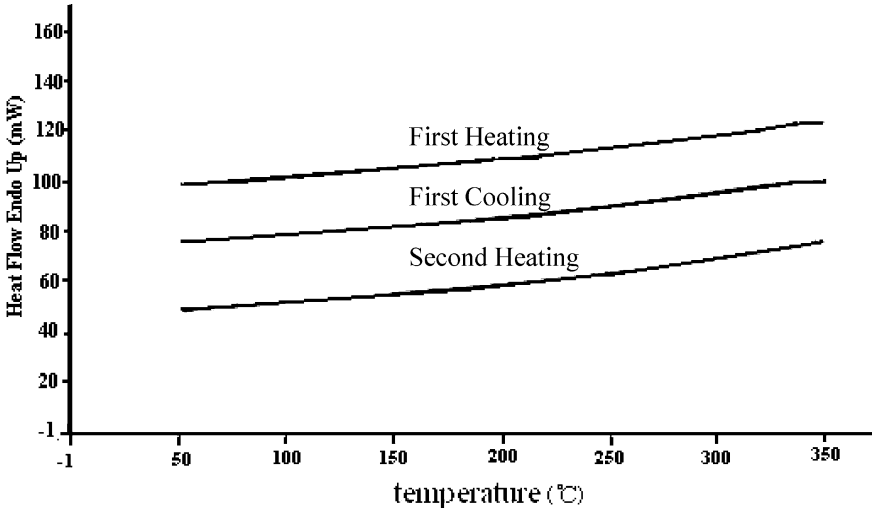

Figure 7. DSC spectra of $Al(Saq)_3$ in cyclic annealing. The heating and cooling rate are the same at 5 °C/min.

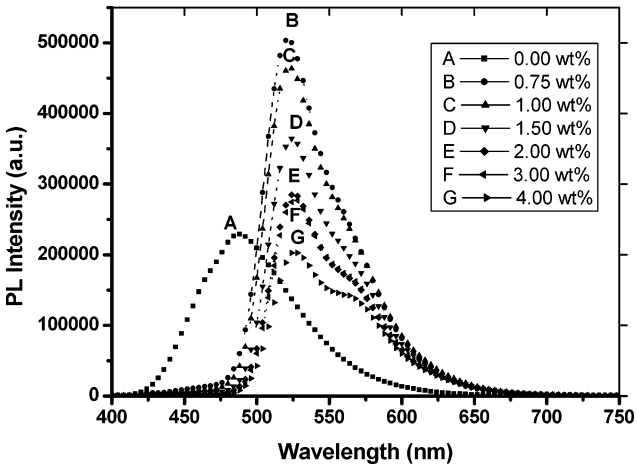

Figure 8. Solid PL of C-545T doped in $Al(Saq)_3$ with various concentrations.

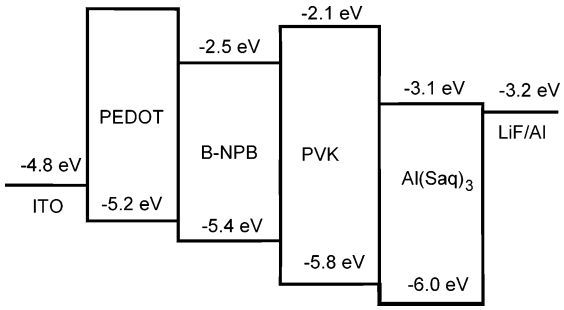

Figure 9. Energy diagram of materials in device fabrication.

Electroluminescence. A single layered device based on this new material was evaluated by the structure of glass/ITO (20 nm)/PEDOT: PSS (70 nm)/$Al(Saq)_3$ (70 nm)/LiF (1 nm)/Al (200 nm). It initially produced a navy blue emission of $CIE_{x,y} = (0.21, 0.41)$ with relatively low luminance efficiency. By examination of the energy band diagram shown in Figure 9, it can be seen that the HOMO energy level of $Al(Saq)_3$ is too low compared to that of the ITO anode to inject the holes into the $Al(Saq)_3$ efficiently. To improve hole injection and lower the HOMO energy barrier between PEDOT and $Al(Saq)_3$, NPB and PVK were used and introduced into the emitting layer of $Al(Saq)_3$. For comparison purpose, single-layer devices with the structure of glass/ITO/PEDOT:PSS (70 nm)/$Al(Saq)_3$ (40 wt %):β-NPB (x wt %): PVK (60-x wt %) (70 nm)/LiF (1 nm)/Al (200 nm) were also made. Figure 10 shows their EL properties. The device (A) with the PVK:$Al(Saq)_3$ blend showed blue-green emission and single peak during electroluminescence process in Figure 10a. Its chromaticity and emission wavelength were also similar to that of the EL spectrum of $Al(Saq)_3$ without PVK. For the I−V curves shown in Figure 10b, the turn-on voltage was droped efficiently with the addition of β-NPB. From EL spectra,

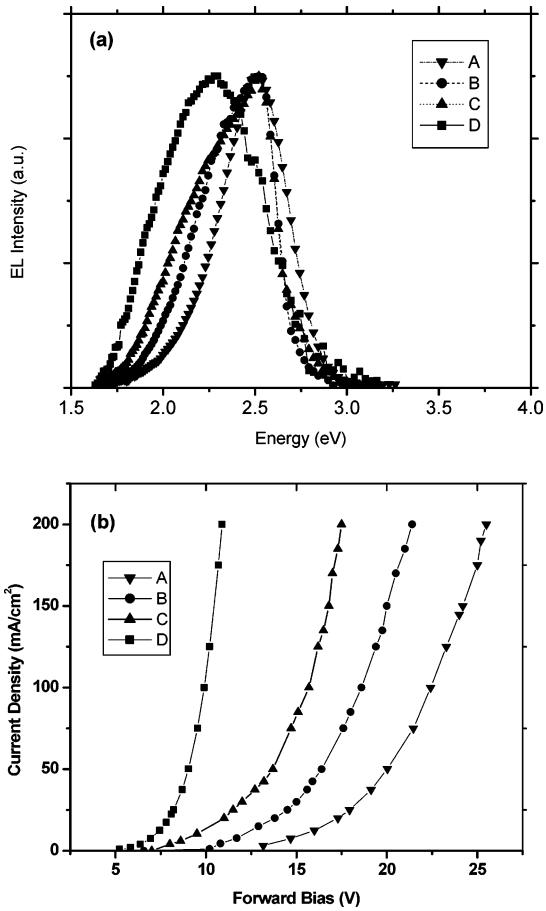

Figure 10. (a) Electroluminescence device glass/ITO/PEDOT:PSS/PVK (60-x wt %):β-NPB(x wt %):$Al(Saq)_3$ (40 wt %)/LiF (1 nm)/Al (200 nm). (b) I−V curves. Device A, $x = 0$; device B, $x = 10$; device C, $x = 20$; device D, $x = 30$.

emission from exciplex at 2.23 eV (556 nm) generated by $Al(Saq)_3$ and β-NPB was observed. By CV measurement, the LUMO and HOMO energy levels of $Al(Saq)_3$ and β-NPB are −3.13 eV, −6.04 eV and −2.50 eV, −5.40 eV, respectively. The difference of energy level between $Al(Saq)_3$'s LUMO and β-NPB's HOMO is around 2.27 eV. By estimation, the exciplex appeared at 2.23 eV which is only 0.04 eV away from 2.27 eV. Therefore, it's highly possible for both holes and electrons to recombine at the $Al(Saq)_3/\beta$-NPB interface, which will cause the emission of orange light as well as efficiency reduction. Furthermore, in the single-layer device, holes and electrons are expected to recombine at the cathode/emitter interface due to mobility and reduce the efficiency of the electroluminescent. Further improvements have been recently obtained by fabricating multilayer devices and will be reported later.

Conclusion

We have synthesized and fabricated one of the first small-molecule, spin-coated single-layer devices based on the novel blue $Al(Saq)_3$ host materials. In single-crystal diffraction and thermal characterization, the meridional form of $Al(Saq)_3$ thin films not only suppresses intermolecular packing, but also exists mainly in amorphous state. Because the IP level is around −6.04 eV, the EL efficiency is poor. It could be enhanced by introducing suitable hole transporting material to inhibit exciplex formation. This type of solution-processible material would be of interest to the OLED community for development of the next generation of small-molecule fabrication technology.

Acknowledgment. We thank Ms. Liao and Ms. Hung, Department of Crystallography, National Tsing-Hua University, Taiwan for single-crystal X-ray measurement. J.-A.C. is grateful to Dr. H. L. Yang of Toppoly Optoelectronics Co. for valuable discussion. This work was supported by NSC and the Ministry of Education of Taiwan, Republic of China (PPAEU 91-E-FA04-2-4-(B)).

CM035313I